International Journal of
Molecular Sciences

MDPI

Article

Expression Profiles and Characteristics of Apple lncRNAs in Roots, Phloem, Leaves, Flowers, and Fruit

Dajiang Wang, Yuan Gao, Simiao Sun, Lianwen Li and Kun Wang *

Research Institute of Pomology, Chinese Academy of Agricultural Sciences (CAAS), Key Laboratory of Horticulture Crops Germplasm Resources Utilization, Ministry of Agriculture and Rural Affairs of the People's Republic of China, Xingcheng 125100, China; dajiang0101@126.com (D.W.); gaoyuan02@caas.cn (Y.G.); sunsimiao@caas.cn (S.S.); lilianwen@caas.cn (L.L.)
* Correspondence: wangkun@caas.cn; Tel.: +86-429-359-8120

Abstract: LncRNAs impart crucial effects on various biological processes, including biotic stress responses, abiotic stress responses, fertility and development. The apple tree is one of the four major fruit trees in the world. However, lncRNAs's roles in different tissues of apple are unknown. We identified the lncRNAs in five tissues of apples including the roots, phloem, leaves, flowers, and fruit, and predicted the intricate regulatory networks. A total of 9440 lncRNAs were obtained. LncRNA target prediction revealed 10,628 potential lncRNA–messenger RNA (mRNA) pairs, 9410 pairs functioning in a cis-acting fashion, and 1218 acting in a trans-acting fashion. Functional enrichment analysis showed that the targets were significantly enriched in molecular functions related to photosynthesis-antenna proteins, single-organism metabolic process and glutathione metabolism. Additionally, a total of 88 lncRNAs have various functions related to microRNAs (miRNAs) as miRNA precursors. Interactions between lncRNAs and miRNAs were predicted, 1341 possible interrelations between 187 mdm-miRNAs and 174 lncRNAs (1.84%) were identified. MSTRG.121644.5, MSTRG.121644.8, MSTRG.2929.2, MSTRG.3953.2, MSTRG.63448.2, MSTRG.9870.2, and MSTRG.9870.3 could participate in the functions in roots as competing endogenous RNAs (ceRNAs). MSTRG.11457.2, MSTRG.138614.2, and MSTRG.60895.2 could adopt special functions in the fruit by working with miRNAs. A further analysis showed that different tissues formed special lncRNA–miRNA–mRNA networks. MSTRG.60895.2–mdm-miR393–MD17G1009000 may participate in the anthocyanin metabolism in the fruit. These findings provide a comprehensive view of potential functions for lncRNAs, corresponding target genes, and related lncRNA–miRNA–mRNA networks, which will increase our knowledge of the underlying development mechanism in apple.

Keywords: apple; lncRNA; tissue–specific expression; regulatory networks; qRT-PCR

Citation: Wang, D.; Gao, Y.; Sun, S.; Li, L.; Wang, K. Expression Profiles and Characteristics of Apple lncRNAs in Roots, Phloem, Leaves, Flowers, and Fruit. *Int. J. Mol. Sci.* **2022**, *23*, 5931. https://doi.org/10.3390/ijms23115931

Academic Editor: Pedro Martínez-Gómez

Received: 24 April 2022
Accepted: 23 May 2022
Published: 25 May 2022

1. Introduction

Long non-coding RNAs (lncRNAs) are a group of poorly conserved RNA molecules that are longer than 200 nucleotides and have no protein encoding abilities [1,2]. They interact with large molecules, such as DNA, RNA, and proteins. Other known functions of lncRNAs consists of regulating protein modification, chromatin remodeling, proteins' functional activity, and RNA metabolism in vivo through cis or trans activation at the transcriptional, post-transcriptional, and epigenetic levels [3]. Most lncRNAs exhibit specific spatial structures and spatiotemporal expression patterns. According to the positions of lncRNAs relative to adjacent protein-coding genes in the genome, lncRNAs can be divided into the following five types: sense lncRNAs, antisense lncRNAs, bidirectional lncRNAs, intronic lncRNAs (incRNAs), and large intergenic lncRNAs (lincRNAs) [4–7].

In plants, lncRNAs are involved in diverse biological processes such as phosphate homeostasis, flowering, photomorphogenesis, the stress response, and fertility [8,9]. As previously reviewed in greater detail, they also play the following important roles: (1) being processed into shorter ncRNAs [10]; (2) acting as both targets and endogenous target mimics

for the miRNAs [11–14]; (3) repressing histone-modifying activities and directing epigenetic silencing through interaction with specific chromatin domains [15–18]; (4) functioning as molecular cargo for protein relocalization [19,20]; and (5) regulating post-translational processes via protein modifications and protein–protein interactions [21].

LncRNAs can function during tissue development, during sexual reproduction, and in response to external stimuli such as drought, salinity, heat stress, and infections in plants [22–26]. *NATs*, *HID1*, *APOLO*, *ASCO*, *COLDAIR*, *COOLAIR* (*Arabidopsis*) [14,16,27–29], *MtENOD40* (*Medicago truncatula*) [19], *LDMAR* (rice) lncRNAs [30,31], which are associated with diverse biological processes, were identified and their physiological functions were initially demonstrated. Most of the knowledge on lncRNAs' regulatory networks was derived from animals and model plants. To date, only a few lncRNA mechanisms have been revealed in apples, so little is known about the systematic and consensus lncRNA regulatory networks. Further research into apple lncRNAs is warranted to elucidate the regulatory networks of the lncRNAs in apples.

In the present study, we identified lncRNAs from five tissues of 'Gala' apples. A total of 9440 lncRNAs were obtained, some of which showed tissue-specific gene expression. The lncRNA–mRNA and lncRNA–miRNA–mRNA interaction-based functional roles showed that these lncRNAs mediated the regulation of photosynthesis-antenna proteins, single-organism metabolic process, glutathione metabolism, and flower coloration. These findings enhance our understanding of the putative regulatory functions of lncRNAs in apple development.

2. Results

2.1. Identification and Characteristics of lncRNAs in 'Gala' Apples

In total, 318.52 Gb of clean data were produced for the RNA-seq from roots, phloem, leaves, flowers, and fruit of 'Gala' apples. After mapping them to the apple reference genome, 147,848,711, 142,596,329, 145,428,347, 127,673,515, and 146,376,167 raw reads corresponding to 119,295,520, 116,145,301, 99,284,229, 104,031,259, and 117,814,110 valid reads were identified in the roots, phloem, leaves, flowers, and fruit from the RNA sequencing (Table S1). On average, the ratio of valid reads, Q30, and GC content in the five libraries were 78.4%, 94.5% and 46.0%, respectively (Table S2).

Not all reads obtained by RNA-seq were lncRNAs, and transcripts longer than 200 nt with at least two exons were selected as lncRNA candidates. Further screened using coding potential calculator (cpc)/coding-non-coding index (cnci)/protein family (pfam)/coding potential assessment tool (cpat) was conducted, which differentiated protein-coding genes from non-coding genes (Figure 1a). A total of 9440 lncRNAs were obtained from the five tissues of 'Gala' apple. Intergenic lncRNAs, sense lncRNAs, antisense lncRNAs and intronic lncRNA accounted for 73.9%, 15.1%, 7.7%, and 3.3% of them, respectively (Table S3 and Figure 1b). The lengths of the lncRNAs ranged from 202 to 10,450 bp. The majority (49.53%) of lncRNA's lengths were around 400–600 bp (Table S4 and Figure 1b).

The Circos plot revealed a non-random distribution of lncRNAs in the chromosomes. Some chromosomal regions had few lncRNAs, and some had a high density of lncRNAs. The lncRNAs were more widely distributed in chromosomes 5, 10, and 15, which accounted for 7.56%, 7.07%, and 6.85%, respectively, while chromosome 14 had the fewest, at 291. Different types of lncRNAs on chromosomes had differences in their distribution characteristics. Sense lncRNAs were mainly distributed at both ends of chromosomes. They had the highest number of lincRNAs and the distribution was dense. Intronic lncRNAs were sparsely distributed on chromosomes, but the distribution density varied greatly in different regions. Antisense lncRNAs generally tended to be located at one end of the chromosome (Table S4 and Figure 1c).

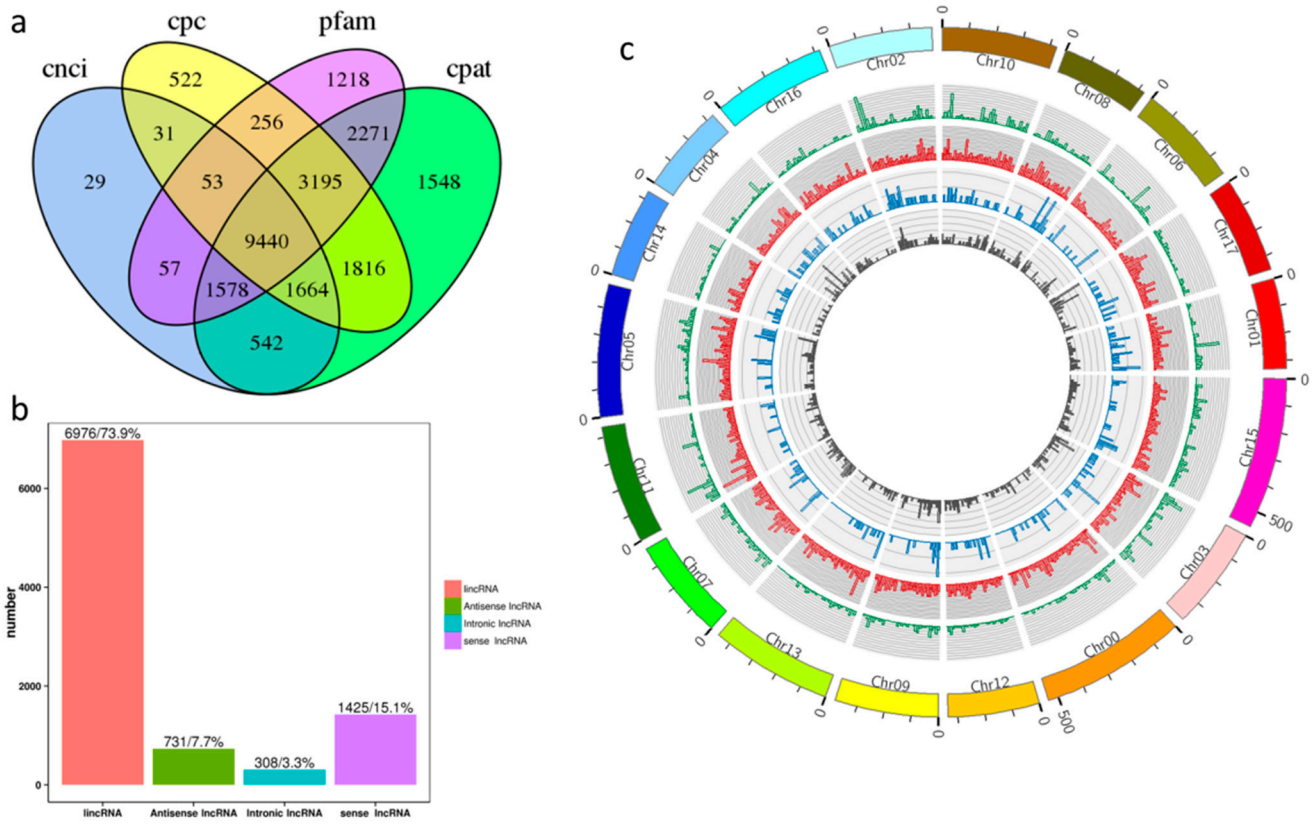

Figure 1. Screening and classification of lncRNAs. (**a**) Results of screening using cnci, cpc, pfam, and cpat. (**b**) Classification of lncRNAs. (**c**) Distribution of lncRNAs identified in chromosomes (green: sense lncRNAs; red: lincRNAs; blue: intronic lncRNAs; grey: antisense lncRNAs).

2.2. Comparative Analysis of mRNAs and lncRNAs

We were able to discover the differences in the structure and sequence of mRNAs and lncRNAs by comparing the lengths, numbers of exons and ORFs. The sequence lengths of the lncRNAs were below 1000 bp, accounting for 70.19% of the total, with most being below 400 bp, while the sequence lengths of the mRNAs were mainly over 3000 bp, accounting for 25.74% (Figure 2a,b). Regarding the number of exons in each lncRNA, most of the lncRNAs had two exons, which accounted for 71.99% of the total; the greatest number of exons in one lncRNA was 15. However, slightly over 5% of mRNAs had only one exon, and a single mRNA could contain more than thirty exons (Figure 2c,d). The ORF lengths of the lncRNAs and mRNAs were predicted, and were concentrated at less than 300 bp. However, the maximum length of the lncRNAs was about 500 bp, while the maximum length of the mRNAs was more than 2000 bp, which was related to their respective average lengths; the lncRNAs themselves were relatively short (Figure 2e,f). By comparing the expression levels of the mRNAs and lncRNAs using an FPKM boxplot of all the transcripts, the expression levels of the two were found to be similar, with low expression levels in most of them and high expression levels in some. On the median line, the mRNA expression was slightly lower than the lncRNA expression (Figure 2g, Tables S4 and S5).

Alternative splicing is a very common phenomenon in eukaryotic plants. The precursor mRNA (pre-mRNA) of a single gene can be processed at different splicing sites to produce multiple mature mRNA subtypes, which is called alternative splicing. About 60% of multi-exon genes can undergo alternative splicing in plants, which plays an important role in plant growth and development. The number of alternative-splicing isomers of the lncRNAs was significantly lower than that of the mRNAs when examining the screened lncRNAs. Overall, 1336 lncRNAs had more than two isomers, with the most being thirty five isomers for one of the lncRNAs; 26,400 mRNAs had more than two isomers. The

highest number of isomers was found for an mRNA with 302 isomers. This indicated that mRNAs had more variable splicing than lncRNAs (Figure 2h).

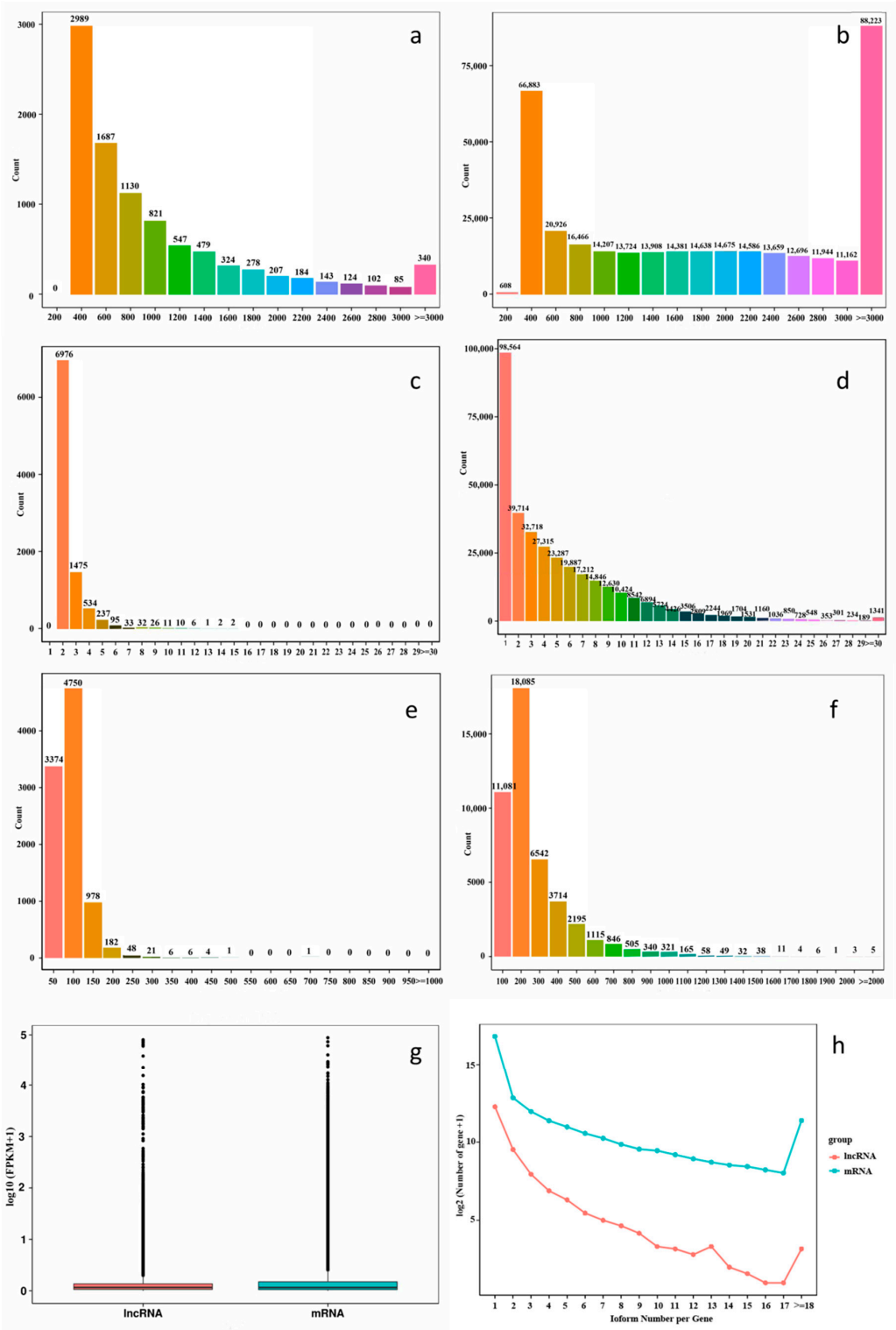

Figure 2. Comparison of the lncRNAs and mRNAs identified. (**a**) Length distribution of the lncRNAs. (**b**) Length distribution of the mRNAs. (**c**) Exon distribution of the lncRNAs. (**d**) Exon distribution of the mRNAs. (**e**) ORF lengths distribution of the lncRNAs. (**f**) ORF lengths distribution of the mRNAs. (**g**) Expression levels of the lncRNAs and mRNAs identified. (**h**) Isoforms of the lncRNAs and mRNAs identified.

2.3. Differential Expression of lncRNAs in Tissues of 'Gala' Apples

To evaluate the prevalence and spatial expression of lncRNAs in 'Gala' apples, we analyzed the expression of lncRNAs in roots, phloem, leaves, flowers, and fruit. The prevalence was relatively low in different tissues. In total, 2676 lncRNAs were shared in the five libraries, while 346, 491, 243, 721, and 184 lncRNAs were expressed only in the roots, phloem, leaves, flowers, and fruit (Table S6 and Figure 3a). We normalized the expression profiles of the 2676 prevalent lncRNAs based on their FPKM values, which permitted us to conduct quantitative comparisons of the levels of lncRNAs among the different tissues. Significant differences among the five tissues were found except between the flowers and leaves; the expression of lncRNAs in the fruit was lower than that in the other tissues (Figure 3b). Interestingly, MSTRG.120812.1, NSTRG.120812.2, MSTRG.120812.3, MSTRG.65728.1, and MSTRG.51285.3 were enriched in all five tissues, the first three of which came from Chr15, and the last two of which came from Chr08 and Chr06. This indicated that these lncRNAs had the important basic functions for different tissues in apples.

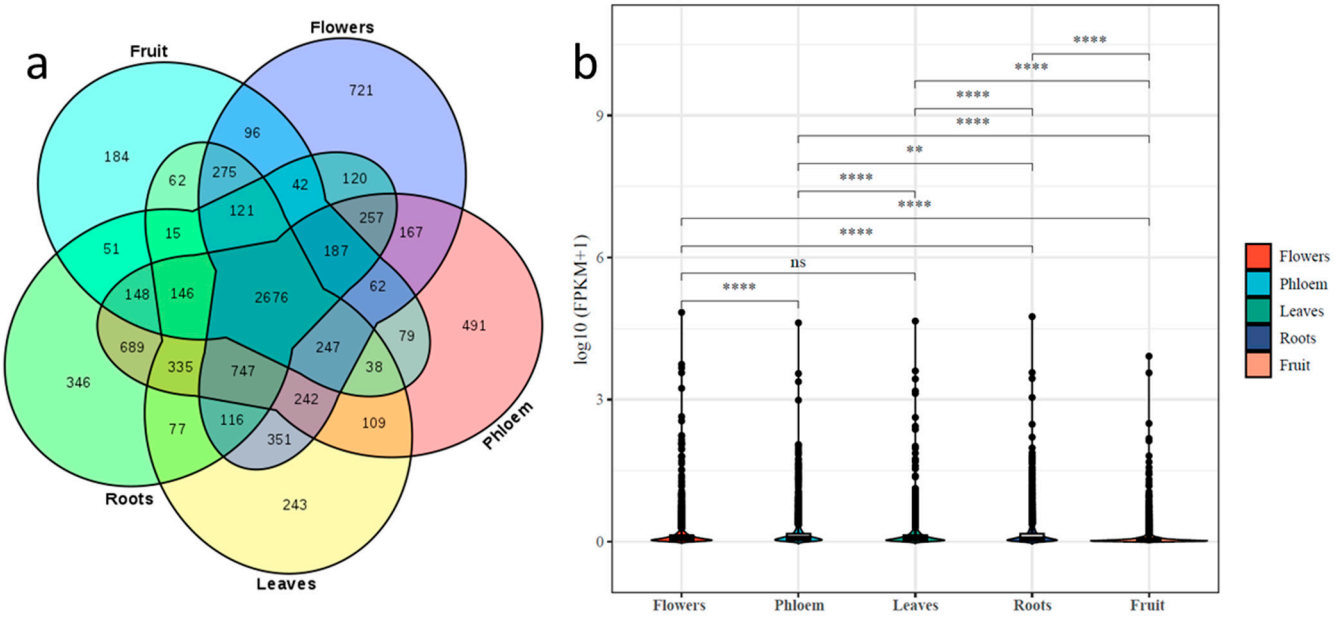

Figure 3. Tissue–specific expression characteristics of the lncRNAs identified. (**a**) Venn diagram showing the number of lncRNAs identified in five tissues of apples. (**b**) The overall abundance patterns of lncRNAs according to FPKM calculations (ns: no significant difference; **: significant difference level at $p < 0.01$; ****: significant difference level at $p < 0.0001$).

2.4. Analysis of miRNA Precursors in lncRNAs

The lncRNAs that were precursors of miRNAs were predicted by comparing them with miRNA sequences in the miRBase database. We identified 88 lncRNAs as potential precursors for 74 miRNAs belonging to 18 families. One lncRNA could act as a precursor for several miRNAs. For example, MSTRG.121641.28 could be a precursor for five members of the mdm-miR156 families. Furthermore, the same miRNA could have more than one precursor. For example, there were 10 lncRNAs that could be precursors for mdm-miR156a (Table S7).

2.5. Target Gene Prediction for lncRNAs

We used two prediction methods based on the interaction modes for lncRNAs and target genes. First, lncRNAs putatively regulate the expression of their neighboring genes, which can be cis-target genes if they are within the 100 kb of the lncRNAs. There were 9410 lncRNAs that were predicted to have one or more target genes, and there were even 44 target genes for one lncRNA (Table S8). Second, in the LncTAR software, complementary

sequences were used between lncRNAs and mRNAs to calculate the pairing site free energy and standardized free energy, and those below the standardized free-energy threshold (<−0.1) were considered to be the trans-target genes of the lncRNAs. There were only 1218 lncRNAs that were predicted to have target genes, many of which only had one target gene, but MSTRG.41634.1 had 39 trans-target genes (Table S9).

2.6. Analysis of Function of lncRNAs

LncRNAs may serve as precursors of miRNAs and also have cis-targeting and trans-targeting relationships with genes. Therefore, it was speculated that lncRNAs can not only play a role in the regulation network for miRNAs but also directly regulate the expression of target genes. In order to understand the possible functions of lncRNAs, we analyzed the tissue-specific networks for miRNA binding and the functions of cis-target and trans-target genes.

Among the 88 lncRNAs that were predicted to be the precursors of miRNAs, 21 were expressed in all five tissues. The results indicated that their functions were relatively common and important. These mainly served as precursors for mdm-miR156, mdm-miR160, mdm-miR164, mdm-miR166, mdm-miR167, mdm-miR171, mdm-miR172, mdm-miR482, mdm-miR535, mdm-miR828, and mdm-miR5225. Two lncRNAs, MSTRG.17430.4 and MSTRG.10845.2, were specifically expressed in the flowers. These two lncRNAs were predicted to be precursors of mdm-miR156 and mdm-miR160, respectively. Six lncRNAs were specifically expressed in the leaves, which were predicted to be precursors of mdm-miR164, mdm-miR167, mdm-miR172, and mdm-miR5225. LncRNA MSTRG.63448.2 was specifically expressed in the roots, which was predicted to be a precursor of mdm-miR156. LncRNA MSTRG.60895.2 was specifically expressed in the fruit, which was predicted to be a precursor of mdm-miR393 and mdm-miR7126.

The GO term enrichment analysis of the differentially expressed cis-target genes and trans-target genes of the lncRNAs in the five tissues allowed us to understand the biological functions of the differentially expressed genes. For the cis-target genes, 30 main functions were selected for analysis, among which the intracellular part was the most enriched, with 1889 genes, but there was no significant difference among the tissues. The expression levels of genes in the GO-term enrichment of single-organism signaling, ribonucleoprotein complex binding, and extracellular organelles showed large differences among the five tissues. For example, the flowers and fruit had a lower expression of single organism signaling, while the phloem had a higher expression level (Figure 4a). The KEGG pathway enrichment analysis showed that there were significant differences in different tissues for photosynthesis-antenna proteins, with the highest expression in the leaves and the lowest in the root. In addition, the phenylalanine metabolism was the highest in the fruit, but lower in other tissues (Figure 4b). For the trans-target genes, there were only three GO-term enrichment clusters, which were as follows: ion binding, single-organism metabolic process, and heterocyclic compound binding. Roots and fruit demonstrated a higher expression of these than the flowers, phloem, and leaves (Figure 4c). Three KEGG pathway enrichments were formed for trans-target genes, including glutathione metabolism, phagosome, and glycosylphosphatidylinositol (GPI)-anchor biosynthesis; the flowers had a higher expression for glutathione metabolism than the others (Figure 4d).

2.7. lncRNA-miRNA Interaction Network in Apples

In order to understand whether lncRNAs could be targets of miRNAs and further affect the post-transcriptional regulation of genes in apples, the potential regulation networks between lncRNAs and miRNAs were predicted. Only the known apple miRNAs and expectation scores ≤ 3 were analyzed here. In total, 1341 possible interrelations between 187 mdm-miRNAs and 174 lncRNAs (1.84%) were predicted. Multiple lncRNAs (or mdm-miRNAs) were predicted to interact with at least one mdm-miRNA (or lncRNA). For example, MSTRG.24932.13 could be targeted by 32 mdm-miRNAs, and mdm-miR172a could target 26 lncRNAs. The mdm-miR156 family had the most target sites (408) in

lncRNAs, followed by the mdm-miR172 family with (370). It indicated that the networks between lncRNAs and miRNAs played a vitally important role in apples, especially for the mdm-miR156 and mdm-miR172 families (Table S10).

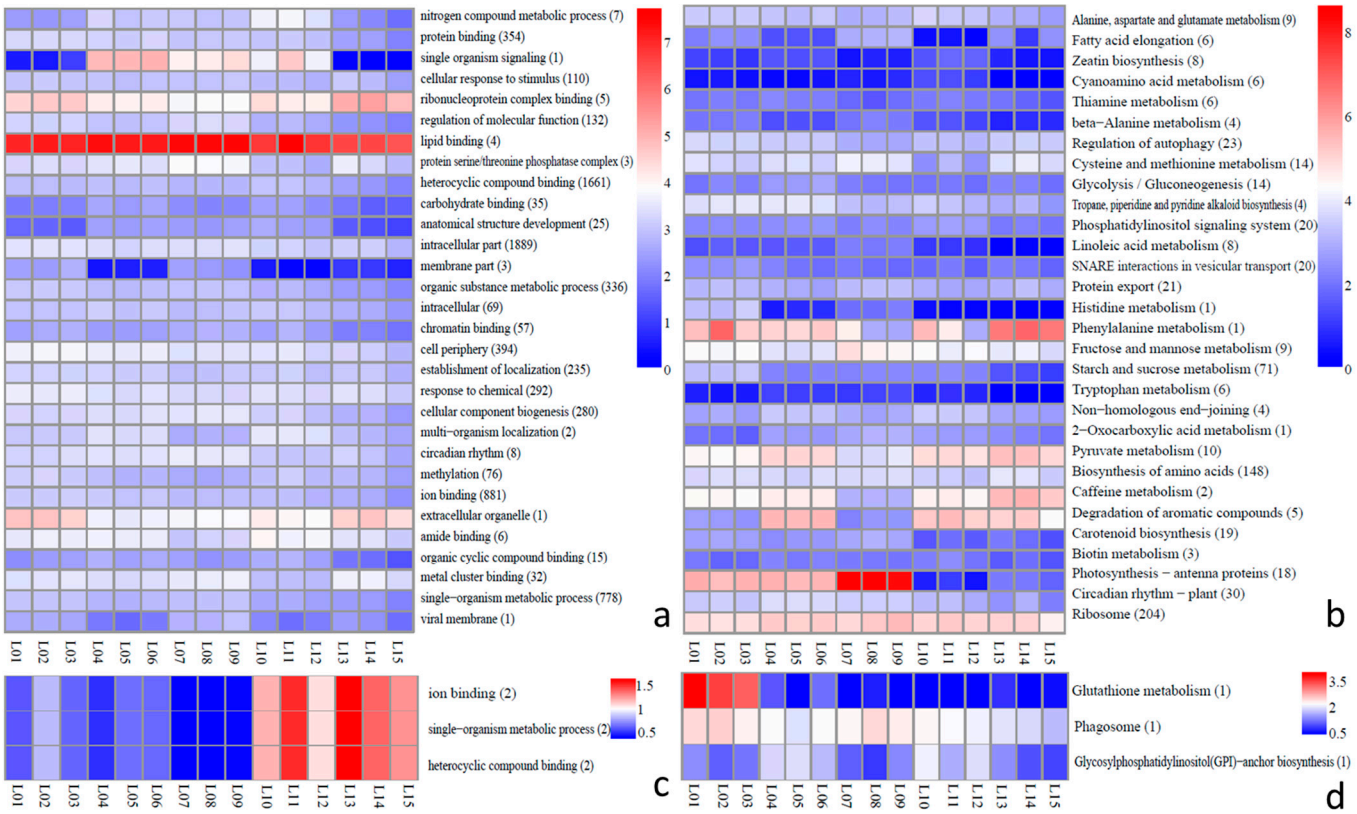

Figure 4. GO term and KEGG pathway enrichment analysis of all differentially expressed of lncRNAs in five tissues (L1–L3: flowers; L4–L6: phloem; L7–L9: leaves; L10–L12: roots; L13–L15: fruit). (**a**) GO term enrichment analysis of all differentially expressed cis-target genes of lncRNAs. (**b**) KEGG pathway enrichment analysis of all differentially expressed cis-target genes of lncRNAs. (**c**) GO term enrichment analysis of all differentially expressed trans-target genes of lncRNAs. (**d**) KEGG pathway enrichment analysis of all differentially expressed trans-target genes of lncRNAs.

Furthermore, miRNAs also had the characteristics of spatial–temporal expression; interactions between lncRNAs and miRNAs were featured to illustrate the functions in different tissues. There were 291 interactions in all five tissues between 26 miRNA families and 55 lncRNAs, including mdm-miR156, mdm-miR164, mdm-miR172, and mdm-miR482. The greatest number of interactions was identified for the mdm-miR156 family, and there were 81 interactions with lncRNAs out of 291 interactions. There were only 71, 1, 111, 41, and 12 interactions in the roots, phloem, leaves, flowers, and fruit, respectively (Figure 5a and Table S11). In particular, the module in a network of MSTRG.121644.5–mdm-miR156, MSTRG.121644.8–mdm-miR156, MSTRG.2929.2–mdm-miR827, MSTRG.3953.2–mdm-miR395, MSTRG.63448.2–mdm-miR156, MSTRG.9870.2–mdm-miR159, and MSTRG.9870.3–mdm-miR159 were only predicted in the roots. MSTRG.11457.2–mdm-miR7126, MSTRG.138614.2–mdm-miR10993, and MSTRG.60895.2–mdm-miR393 were only predicted in the fruit. They may have special expression and regulation characteristics in these tissues.

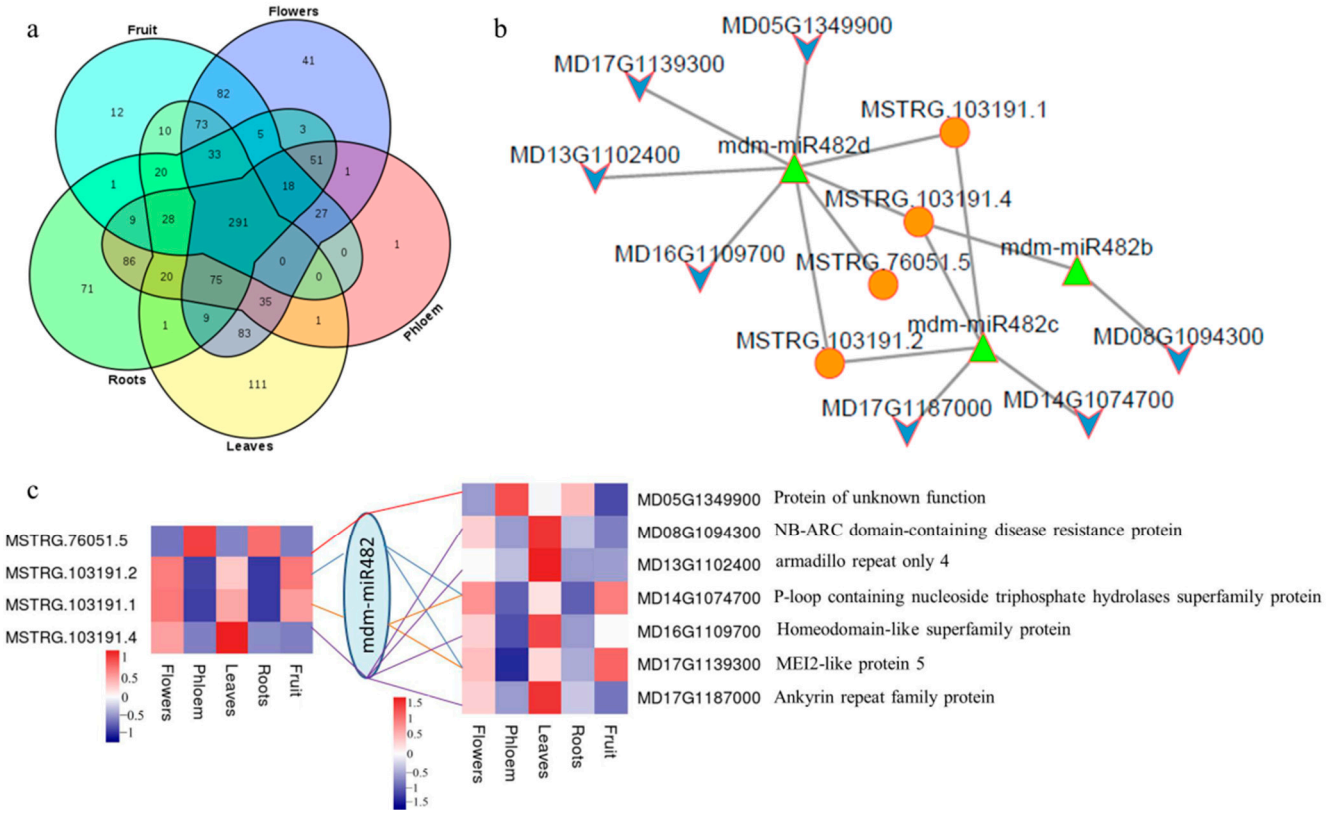

Figure 5. Tissue-specific characteristics and functions, and prediction of lncRNA-miRNA-mRNA. (**a**) Venn diagram of interactions between lncRNAs and miRNAs of five tissues. (**b**) lncRNA-miRNA-mRNA networks for mdm-miR482 (orange circle: lncRNAs; green triangle: mdm-miRNAs; blue arrow: mRNAs). (**c**) Pearson correlation coefficient for expression of lncRNAs and mdm-miR482 in five tissues and functions of mRNAs.

In order to further reveal the potential functions of lncRNAs, lncRNA–miRNA–mRNA networks were constructed. We analyzed the correlation of the expression of lncRNAs and mRNAs in five tissues. The expression of lncRNAs and mRNAs targeted by miRNAs should be positively correlated. We extracted lncRNAs and mRNAs whose correlation coefficients were greater than 0.8 with a significance level of 0.05 (Table S12); then, regulatory network diagrams were constructed (Figure 5b and Figures S1–S5) and the possible role of the lncRNA was speculated on through the functional annotation of mRNAs. As Figure 5c showed, the expression of four lncRNAs and seven mRNAs was highly positively correlated in five tissues. They were targeted by the mdm-miR482 family, which participated in the anti-stress response in apples. Thus, MSTRG.76051.5, MSTRG.103191.1, MSTRG.103191.2, and MSTRG.103191.4 may play a major role in resistance for apples. In addition, other lncRNAs had special roles in different tissues of the apple. For example, MSTRG.60895.2 may participate in the anthocyanin metabolism in fruit by competing with MD17G1009000 as a target of mdm-miR393, whose auxin signaling F-box 2 was associated with anthocyanin metabolism (Table S12).

2.8. qRT-PCR Validation

To confirm our identification of lncRNAs, four random lncRNA candidates were selected for experimental validation using a quantitative reverse transcription PCR (qRT-PCR). The primers were designed based on sequences on both sides of the candidate lncRNAs. As shown in Figure 6, in this study, four randomly selected lncRNAs all showed expression patterns consistent with the RNA-seq results. The R squared values for the RNA-seq vs. qRT-PCR were 0.6137, 0.8999, 0.8593 and 0.9567 for MSTRG.121641.28, MSTRG.121641.3,

MSTRG.121644.1 and MSTRG.10845.1, respectively. The results indicated that the lncRNAs identified in the RNA-seq datasets were reliable.

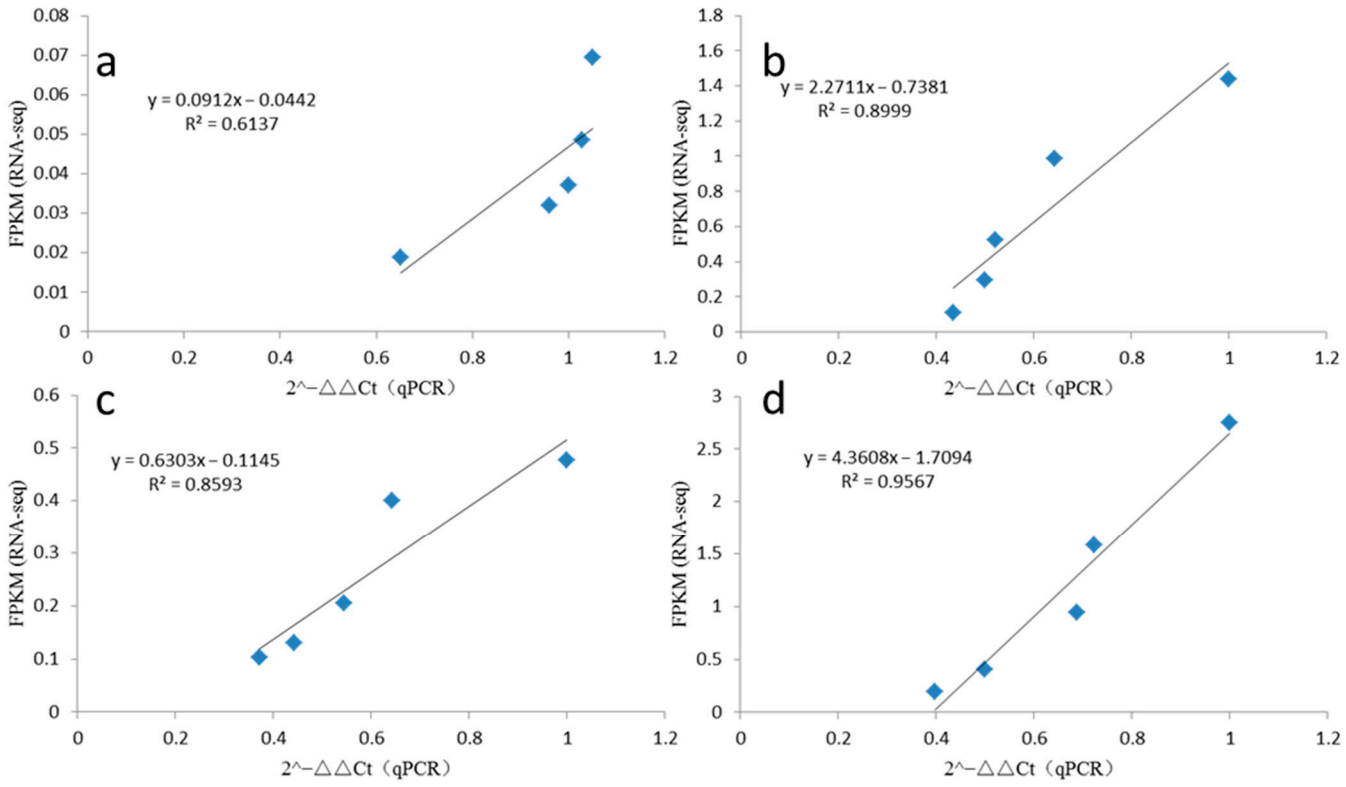

Figure 6. The linear relationship between RNA-seq and qRT-PCR data ((**a**–**d**) were MSTRG.121641.28, MSTRG.121641.3, MSTRG.121644.1, and MSTRG.10845.1, respectively).

3. Discussion

LncRNAs show organ, developmental and environmental expression specificity in plants [32–34]. Thousands of plant lncRNAs have been identified, and some of their molecular functions have been studied [18,22,29,35–38], but only a few studies have been conducted for apples [7,39]. Here, we reported a genome-wide identification and potential function analysis of the lncRNAs in the roots, phloem, leaves, flowers, and fruit of 'Gala' apples. Compared with the mRNAs, the lengths of most of the lncRNAs were below 1000 bp, shorter than the mRNAs, and the lncRNAs had fewer exons than the mRNAs, which was consistent with other plants [40,41]. The alternative splicing of mRNAs was more common than that of lncRNAs, the main reason for which may be that the number of exons in the mRNAs was greater than the numbers in lncRNAs.

Studies have indicated that lncRNAs exhibit tissue–specific expression patterns in plants [34,42]. Here, we compared the expression of lncRNAs in five tissues of 'Gala' apple; the expression of lncRNAs showed tissue–specific expression. The numbers of lncRNAs identified in different tissues were different, with the highest in the flowers and the lowest in the fruit, which was consistent with the differential functions and organizations of the tissues. Even the co-expressed lncRNAs in the five tissues showed significant differences in their expression levels, indicating that the same lncRNAs had different functions in different tissues, or their contributions to the function were different. It was interesting that the expression levels in the leaves and flowers had no significant differences. This was because the expression levels of several lncRNA were higher in leaves and in flowers, but were lower in other three tissues. In particular, the FPKM of MSTRG.51285.3 in leaves and flowers was 2708.85 and 3666.36, but it was 73.56, 297.62, and 28.80 in phloem, roots, and fruit, respectively. The FPKM of MSTRG.51285.3 accounted for 4.16%, 0.14%, 4.72%, 0.44%, and 0.22% of the total FPKM of 2676 lncRNAs in flowers, phloem, leaves, roots, and

fruits, respectively. Unfortunately, we did not obtain its function annotation, either on the regulation of genes or on the interaction with miRNAs. It may work in other ways, and it is worth further exploring its functionality.

An lncRNA mainly regulates its target genes in two ways. One is the cis-regulation of neighboring genes, and the other is the trans-regulation of genes with complementary sequences [43,44]. *DROUGHT INDUCED* lncRNA (DRIR) enhanced drought and salt stress tolerance in *Arabidopsis thaliana* by regulating the expression of genes involved in abscisic acid (ABA) signaling, water transport, and stress relief processes [45]. Obviously, in this study, there were more cis-target genes than trans-target genes. The tissue specificity of the cis-target genes was consistent with that of lncRNAs, since the positively regulated genes were near lncRNAs. However, the target genes subjected to trans–regulation were different, and the trans-target genes were predicted based on complementary sequences, which could better highlight the organization orientation and function. The leaves had the highest level of expression for photosynthesis-antenna proteins, which were located on the thylakoid membranes in the chloroplast, and captured light energy which was transferred to the photosynthetic reaction center [46], although there were low levels in the roots. This aligned with the photosynthetic function of leaves. This suggested that lncRNAs may play an important role in photosynthesis. Two lncRNAs, *COOLAIR* and *COLDAIR*, were found to be present in the locus of *FLC* genes and to critically regulate the *FLC* genes' expression by transcriptional regulation and histone modification, respectively [16,27]. The flowers had the highest expression for glutathione metabolism. Previous research showed that flowering was promoted by increasing endogenous glutathione [47]. Hence, lncRNAs may interact with glutathione metabolism to improve flowering in apples.

LncRNAs can act as precursors for miRNAs and play a regulatory role through miRNA production. Both miRNAs and lncRNAs have tissue-specific functions. The genome-scale RNA-seq analysis of flower and fruit tissues from *Fragaria vesca* proved that lncRNAs exhibited tissue-specific expression [48]. Of the 2676 prevalent lncRNAs, 21 can serve as precursors for miRNAs, mainly including the mdm-miR156, mdm-miR160, mdm-miR164, mdm-miR166, mdm-miR167, mdm-miR482 families, and other families, indicating that the role of these 21 lncRNAs as miRNA precursors was universal. Regarding tissue-specific lncRNAs, MSTRG.17430.4 and MSTRG.10845.2 were specifically expressed in flowers and predicted to be precursors of mdm-miR156 and mdm-miR160, respectively. MiR156 plays an important role in the flowering of plants [49]. LincRNAs can act as precursors of small RNAs and regulate diverse metabolic pathways. They can alter miRNA expression by interacting with the corresponding miRNAs [50]. It was speculated that MSTRG.17430.4 had a regulatory effect on flowering. Mdm-miR160 could regulate anthocyanin metabolism. The overexpression of mdm-miR160 reduced the content of anthocyanin in flowers [51]. Consequently, MSTRG.10845.2 may play an important role in flower coloration. The present findings suggested that miR156 regulated root development, nitrogen-fixation activity, and root biomass levels [52–54]. MSTRG.63448.2 was predicted to be a precursor of mdm-miR156 in the roots, and miR156 regulates a network of downstream genes to affect the growth and development of roots.

LncRNAs and miRNAs interact with each other, imposing an additional level of post-transcriptional regulation. LncRNAs can compete with mRNAs for miRNA molecules, promoting the regulation of miRNA-mediated target repression. This type of ceRNA crosstalk has been widely observed in different biological processes and diseases [12,55–57]. In this study, 1341 possible interrelations between 187 mdm-miRNAs and 174 lncRNAs (1.84%) were predicted. The sequences of the binding sites of the lncRNAs were found to be conserved. Thus, a single lncRNA can effectively bind to multiple miRNAs [58]. Multiple lncRNAs (or mdm-miRNAs) were predicted to interact with more than one mdm-miRNA (or lncRNA). *INDUCED BY PHOSPHATE STARVATION 1* (*IPS1*) was a classic example of a functionally characterized cytoplasmic lncRNA that acts via target mimicry to sequester miR-399, which canonically targeted *PHOSPHATE2* (*PHO2*) mRNA [12]. Our study showed similar results, whereby the mdm-miR156 family had the most interactions with lncRNAs

in all five tissues. MiR156 played an important role in plant development, anabolism and abiotic stress, and was a regulatory hub for plant growth and development [59,60]. Therefore, specific lncRNAs may play a major role in the apple's different tissues during its life through ceRNAs for the mdm-miR156 family. It was worth noting that there were more interactions in the roots between mdm-miR156 and lncRNAs than those in fruit. MiR156 involved biotic and abiotic stress in the roots [61–63] and fruit ripening [64,65], whereas lncRNAs–mdm-miR156 networks played a broader role in the roots than in the fruit in apples.

LncRNAs and miRNAs reveal spatiotemporal expression specificity [41,66], with specific networks playing a particular role in organization. There were some interactions predicted only in specific tissues. For example, interactions between some lncRNAs and the mdm-miR156, mdm-miR159, mdm-miR395, mdm-miR827 families were only predicted in the roots. Regarding the functionalities of these families, mdm-miR156 was identified as a positive regulator of drought resistance in apples [67]. MiR159 was identified as a post-transcriptional repressor of primary root growth in *Arabidopsis thaliana* [68]. Mi395 was identified as a general component of the sulfate assimilation regulatory network in *Arabidopsis* [69]. MiR827 could enhance drought tolerance in transgenic barley [70]. All of these involved functions in roots; therefore, we concluded that MSTRG.121644.5, MSTRG.121644.8, MSTRG.2929.2, MSTRG.3953.2, MSTRG.63448.2, MSTRG.9870.2, and MSTRG.9870.3, which were only expressed in roots and interacted with miRNAs, could participate in the functions of roots as ceRNAs. In the same way, mdm-miR393, mdm-miR7126, and mdm-miR10993 interacted with miRNAs only in the fruit, although miR393 could regulate fruit/seed set development in cucumbers [71]. *MdARF3* (MD17G1009000) was reported to negatively regulate anthocyanin anabolism as a fast auxin response factor [72]. We had reason to speculate that MSTRG.60895.2–mdm-miR393–MD17G1009000 may participate in the anthocyanin metabolism in the fruit of apples.

4. Materials and Methods

4.1. Plant Materials

The materials of the phloem, leaves, flowers, and fruit were collected from the 'Gala' apples. The scion of 'Gala' was grafted on *Malus baccata* (L.) Borkh. in 2001, and the tree was planted in the field of the National Repository of Apple Germplasm Resources (Xingcheng) in 2002. The roots were harvested from the tissue culture plantlets. All the materials were frozen using liquid nitrogen and stored at −80 °C. Each line had three biological replicates.

4.2. RNA Isolation, Quantification and Qualification

Total RNA was isolated from each sample using the plant RNA isolation kit (Aidlab Company, Beijing, China) according to the manufacturer's instructions. rRNA was removed using the Epicenter Ribo-Zero^{TM} (Epicentre, Madison, WI, USA) following the manufacturer's procedure. RNA degradation and contamination, especially DNA contamination, were monitored on 1.5% agarose gels. The RNA concentration and purity were measured by using the NanoDrop 2000 Spectrophotometer (Thermo Fisher Scientific, Wilmington, DE, USA). The RNA integrity was assessed by using the RNA Nano 6000 Assay Kit of the Agilent Bioanalyzer 2100 System (Agilent Technologies, Santa Clara, CA, USA).

4.3. Library Preparation for lncRNA-Seq

A total of 1.5 μg of RNA per sample was used as input material for rRNA removal by using the Ribo-Zero rRNA Removal Kit (Epicentre, Madison, WI, USA). Sequencing libraries were generated by using the NEBNext^{R} Ultra^{TM} Directional RNA Library Prep Kit for Illumina^{R} (NEB, Ipswich, MA, USA) following the manufacturer's recommendations and index codes were added to attribute sequences to each sample. Briefly, fragmentation was carried out using divalent cations under high temperature in NEBNext First Strand Synthesis Reaction Buffer (5x). First-strand cDNA was synthesized using random hexamer primers and reverse transcriptase. Second-strand cDNA synthesis was subsequently per-

formed using DNA Polymerase I and RNase H. Remaining overhangs were converted into blunt ends via exonuclease/polymerase activities. After the adenylation of the 3′ ends of the DNA fragments, the NEBNext Adaptor with a hairpin loop structure was ligated to prepare for hybridization. In order to select insert fragments, preferentially of 150~200 bp in length, the library fragments were purified with AMPure XP Beads (Beckman Coulter, Beverly, MA, USA). Then, 3 µL of USER Enzyme (NEB, Ipswich, MA, USA) was used with size-selected, and adapter-ligated cDNA at 37 °C for 15 min before PCR. Then, PCR was performed with Phusion High-Fidelity DNA polymerase, Universal PCR primers and an Index(X) Primer. Finally, the PCR products were purified byAMPure XP system (Beckman Coulter, Beverly, MA, USA) and the library quality was assessed on the Agilent Bioanalyzer 2100 (Agilent Technologies, Santa Clara, CA, USA) and by qPCR.

4.4. Clustering and Sequencing

The index-coded samples were clustered using the acBot Cluster Generation System with the TruSeq PE Cluster Kitv3-cBot-HS (Illumina, NEB, Ipswich, MA, USA) according to the manufacturer's instructions. After cluster generation, the library preparations were sequenced on an Illumina Hiseq platform, and paired-end reads were generated.

4.5. Quality Control

The raw data (raw reads) of FASTQ format were first processed through in-house Perl scripts. In this step, the clean data (clean reads) were obtained by removing adapters from reads, reads containing ploy-N, and low quality reads from the raw data. At the same time, the Q30, GC content, and sequence duplication level of the clean data were calculated. All the downstream analyses were based on clean data with high quality.

4.6. LncRNA Analysis

The transcriptome was assembled using StringTie based on the reads mapped to the reference genome (*Malus* × *domestica* GDDH13 v1.1) (www.rosaceae.org, accessed on 16 May 2022). The assembled transcripts were annotated using the GffCompare program. The unknown transcripts were used to screen for putative lncRNAs. Four computational approaches including cpc/cnci/pfam/cpat were combined to sort non-protein coding RNA candidates from putative protein-coding RNAs in the unknown transcripts. Putative protein-coding RNAs were removed using a minimum length and exon number threshold. Transcripts longer than 200 nt and with at least two exons were selected as lncRNA candidates and further screened using cpc/cnci/pfam/cpat, which has the power to distinguish protein-coding genes from non-coding genes. Furthermore, different types of lncRNAs including lincRNAs, intronic lncRNAs, antisense lncRNAs, and sense lncRNAs were selected using Cuffcompare (http://cole-trapnell-lab.github.io/cufflinks/cuffcompare/index.html, accessed on 16 May 2022).

4.7. Quantification of Gene Expression Levels

StringTie (1.3.1) (https://ccb.jhu.edu/software/stringtie/index.shtml, accessed on 16 May 2022) was used to calculate the FPKMs of both the lncRNAs and coding genes in each sample [73]. The gene FPKMs were computed by summing the FPKMs of the transcripts in each gene group. The FPKM, which means fragments per kilo-base of exon per million fragments mapped, was calculated based on the lengths of the fragments and the reads count mapped to these fragment.

4.8. Differential Expression Analysis

The differential expression analysis of two conditions/groups was performed using the DESeq R package (1.10.1) (http://www.bioconductor.org/packages/release/bioc/html/DESeq.html, accessed on 16 May 2022). DESeq provides statistical routines for determining differential expression in digital gene expression data using a model based on the negative binomial distribution. The resulting *p*-values were adjusted using the Benjamini–Hochberg

approach for controlling the false-discovery rate. Genes with adjusted p-values < 0.01 and absolute values of log2 (Fold change) > 1 as determined by DESeq were assigned as differentially expressed.

4.9. Gene Functional Annotation

Gene functions were annotated based on the following databases:

Nr (NCBI non-redundant protein sequences).
Pfam (Protein family).
KOG/COG (Clusters of Orthologous Groups of proteins).
Swiss-Prot (a manually annotated and reviewed protein sequence database).
KEGG (Kyoto Encyclopedia of Genes and Genomes).
GO (Gene Ontology).
GO enrichment analysis of the differentially expressed genes (DEGs) was implemented using the topGO R packages.

We used the KOBAS [74] software to test the statistical enrichment of differentially expressed genes in KEGG pathways.

The sequences of the DEGs were blast (blastx) to the genome of a related species (the protein–protein interactions which exist in the STRING database: http://string-db.org/, accessed on 16 May 2022) to obtain the predicted PPI of these DEGs. Then, the PPIs of these DEGs were visualized in Cytoscape [75].

4.10. Prediction of miRNA Target Sites in lncRNAs

We identified the targets of miRNAs using TargetFinder, based on the known miRNAs of apples, the newly predicted miRNAs, and the gene sequence information for 'Golden delicious'. Interactions between lncRNAs and miRNAs with expectation score ≤ 3 were selected. As lncRNAs contain multiple miRNA binding sites, the miRNA target gene prediction methods can be used to identify the lncRNAs that bind to miRNAs, and the functions of lncRNAs can be elucidated based on the functional annotation of the miRNA target genes.

4.11. Quantitative Real-Time PCR Validation

Quantitative real-time PCR (qRT-PCR) was carried out to validate the levels of differential expressional lncRNAs from 'Gala' apples. According to the instructions of the TruScript First-strand cDNA SYNTHESIS Kit (Aidlab Company, Beijing, China), 800 ng of the total RNA was reverse-transcribed with random primers. The reaction system included 800 ng of RNA, 4 µL of 5 × RT Reaction Mix, 0.5 µL of rondam primers/oligodT, 0.5 µL N6, 0.8 µL of TruScript H^- RTase/RI Mix, and RNase free dH_2O was added to obtain a 20 µL volume; the reaction conditions were 42 °C for 40 min and 65 °C for 10 min.

Primers were designed in order to obtain the amplicon from the template (Table S13). Quantitative real-time PCR (qRT-PCR) was performed using SYBR Green Master Mix (Vazyme, Nanjing, China). The qRT-PCR aliquot contained 1 µL of cDNA, 3 µL of ddH_2O, 0.5 µL of each of the forward and reverse primers (200 nM), and 5 µL of 2 × SYBR® Green Supermix. The reaction conditions included initial denaturation at 95 °C for 3 min, followed by 39 cycles at 95 °C for 10 s, and 60 °C for 30 s, with melt curve analysis (60~95 °C, +1 °C/cycle; holding time: 4 s). The levels of the lncRNAs were normalized to *q*Actin. All the real-time PCR assays were performed with three biological replicates. The relative expression levels were calculated with the $2^{-\Delta\Delta Ct}$ method [76].

5. Conclusions

We identified lncRNAs in five tissues of the 'Gala' apple, a variety widely cultivated worldwide. A total of 9440 unique lncRNAs were identified from the leaves, phloem, flower, fruit, and roots. Cis-target and trans-target genes prediction for lncRNAs showed that the target genes were significantly enriched in molecular functions related to photosynthesis-antenna proteins, single-organism metabolic process and glutathione metabolism. In

total, 88 lncRNAs were predicted to be precursors of miRNAs. A total of 1341 possible interrelations between 187 mdm-miRNAs and 174 lncRNAs (1.84%) were predicted when performing a search across the miRNAs of *Malus* in miRBase. It was predicted that MSTRG.121644.5, MSTRG.121644.8, MSTRG.2929.2, MSTRG.3953.2, MSTRG.63448.2, MSTRG.9870.2 and MSTRG.9870.3 could participate in the functions of roots as ceRNAs. MSTRG.11457.2, MSTRG.138614.2 and MSTRG.60895.2 could adopt special functions in the fruit by working with miRNAs. Potential lncRNA–miRNA–mRNA networks were constructed, and the possible roles of lncRNAs in different tissues were considered. We had reason to surmise that MSTRG.60895.2 might participate in anthocyanin metabolism in the fruit by competing with MD17G1009000 as a target for mdm-miR393.

Supplementary Materials: The following supporting information can be downloaded at: https://www.mdpi.com/article/10.3390/ijms23115931/s1.

Author Contributions: D.W. and K.W. planned and designed the experiments; methodology, D.W.; Y.G. and S.S. performed the experiments and used the software; L.L. field management; D.W. analyzed the data and wrote the manuscript; K.W. reviewed and edited the final manuscript. All authors have read and agreed to the published version of the manuscript.

Funding: This research was partly funded by the Agricultural Science and Technology Innovation Program (CAAS-ASTIP-2021-RIP-02).

Institutional Review Board Statement: Not applicable.

Informed Consent Statement: Not applicable.

Data Availability Statement: The raw sequence data reported in this paper have been deposited in the Genome Sequence Archive (Genomics, Proteomics and Bioinformatics 2021) in National Genomics Data Center (Nucleic Acids Res 2022), China National Center for Bioinformation/Beijing Institute of Genomics, Chinese Academy of Sciences (GSA: CRA006669) that are publicly accessible at https://ngdc.cncb.ac.cn/gsa (accessed on 15 March 2022).

Acknowledgments: We would like to thank OmicShare tools, a free online platform for plotting (https://www.omicshare.com/tools, accessed on 12 April 2022), the openbiox community, and the Hiplot team (https://hiplot.com.cn, accessed on 16 May 2022) for providing technical assistance and valuable tools for data analysis and visualization.

Conflicts of Interest: The authors declare no conflict of interest.

References

1. Chen, X. Small RNAs and Their Roles in Plant Development. *Annu. Rev. Cell Dev. Biol.* **2009**, *25*, 21–44. [CrossRef] [PubMed]
2. Rinn, J.L.; Chang, H.Y. Genome Regulation by Long Noncoding RNAs. *Annu. Rev. Biochem.* **2012**, *81*, 145–166. [CrossRef]
3. Wu, L.; Liu, S.; Qi, H.; Cai, H.; Xu, M. Research Progress on Plant Long Non-Coding RNA. *Plants* **2020**, *9*, 408. [CrossRef] [PubMed]
4. Ponting, C.P.; Oliver, P.L.; Reik, W. Evolution and Functions of Long Noncoding RNAs. *Cell* **2009**, *136*, 629–641. [CrossRef] [PubMed]
5. Chekanova, J.A. Long non-coding RNAs and their functions in plants. *Curr. Opin. Plant Biol.* **2015**, *27*, 207–216. [CrossRef]
6. Mattick, J.S.; Rinn, J. Discovery and annotation of long noncoding RNAs. *Nat. Struct. Mol. Biol.* **2015**, *22*, 5–7. [CrossRef]
7. Sun, Y.; Hao, P.; Lv, X.; Tian, J.; Wang, Y.; Zhang, X.; Xu, X.; Han, Z.; Wu, T. A long non-coding apple RNA, MSTRG.85814.11, acts as a transcriptional enhancer of *SAUR32* and contributes to the Fe-deficiency response. *Plant J.* **2020**, *103*, 53–67. [CrossRef]
8. Liu, D.; Mewalal, R.; Hu, R.; Tuskan, G.A.; Yang, X. New technologies accelerate the exploration of non-coding RNAs in horticultural plants. *Hortic. Res.* **2017**, *4*, 17031. [CrossRef]
9. Yuan, J.; Li, J.; Yang, Y.; Tan, C.; Zhu, Y.; Hu, L.; Qi, Y.; Lu, Z.J. Stress-responsive regulation of long non-coding RNA polyadenylation in *Oryza sativa*. *Plant J.* **2017**, *93*, 814–827. [CrossRef]
10. Ben Amor, B.; Wirth, S.; Merchan, F.; Laporte, P.; D'Aubenton-Carafa, Y.; Hirsch, J.; Maizel, A.; Mallory, A.; Lucas, A.; Deragon, J.M.; et al. Novel long non-protein coding RNAs involved in *Arabidopsis* differentiation and stress responses. *Genome Res.* **2008**, *19*, 57–69. [CrossRef]
11. Aung, K.; Lin, S.-I.; Wu, C.-C.; Huang, Y.-T.; Su, C.-L.; Chiou, T.-J. *pho2*, a phosphate overaccumulator, is caused by a nonsense mutation in a microRNA399 target gene. *Plant Physiol.* **2006**, *141*, 1000–1011. [CrossRef]

12. Franco-Zorrilla, J.M.; Valli, A.; Todesco, M.; Mateos, I.; Puga, M.I.; Somoza, I.R.; Leyva, A.; Weigel, D.; Garcia, J.A.; Paz-Ares, J. Target mimicry provides a new mechanism for regulation of microRNA activity. *Nat. Genet.* **2007**, *39*, 1033–1037. [CrossRef] [PubMed]
13. Pant, B.D.; Buhtz, A.; Kehr, J.; Scheible, W.-R. MicroRNA399 is a long-distance signal for the regulation of plant phosphate homeostasis. *Plant J.* **2007**, *53*, 731–738. [CrossRef]
14. Bardou, F.; Ariel, F.; Simpson, C.G.; Romero-Barrios, N.; Laporte, P.; Balzergue, S.; Brown, J.W.; Crespi, M. Long Noncoding RNA Modulates Alternative Splicing Regulators in Arabidopsis. *Dev. Cell* **2014**, *30*, 166–176. [CrossRef] [PubMed]
15. Sheldon, C.C.; Rouse, D.T.; Finnegan, E.J.; Peacock, W.J.; Dennis, E.S. The molecular basis of vernalization: The central role of FLOWERING LOCUS C (FLC). *Proc. Natl. Acad. Sci. USA* **2000**, *97*, 3753–3758. [CrossRef] [PubMed]
16. Heo, J.B.; Sung, S. Vernalization-Mediated Epigenetic Silencing by a Long Intronic Noncoding RNA. *Science* **2011**, *331*, 76–79. [CrossRef] [PubMed]
17. Zhu, Q.-H.; Wang, M.-B. Molecular Functions of Long Non-Coding RNAs in Plants. *Genes* **2012**, *3*, 176–190. [CrossRef] [PubMed]
18. Marquardt, S.; Raitskin, O.; Wu, Z.; Liu, F.; Sun, Q.; Dean, C. Functional Consequences of Splicing of the Antisense Transcript COOLAIR on FLC Transcription. *Mol. Cell* **2014**, *54*, 156–165. [CrossRef]
19. Campalans, A.; Kondorosi, A.; Crespi, M. *Enod40*, a Short Open Reading Frame–Containing mRNA, Induces Cytoplasmic Localization of a Nuclear RNA Binding Protein in *Medicago truncatula*. *Plant Cell* **2004**, *16*, 1047–1059. [CrossRef]
20. Dey, M.; Complainville, A.; Charon, C.; Torrizo, L.; Kondorosi, A.; Crespi, M.; Datta, S. Phytohormonal responses in enod40-overexpressing plants of Medicago truncatula and rice. *Physiol. Plant.* **2004**, *120*, 132–139. [CrossRef]
21. Liu, J.; Wang, H.; Chua, N.-H. Long noncoding RNA transcriptome of plants. *Plant Biotechnol. J.* **2015**, *13*, 319–328. [CrossRef] [PubMed]
22. Xin, M.; Wang, Y.; Yao, Y.; Song, N.; Hu, Z.; Qin, D.; Xie, C.; Peng, H.; Ni, Z.; Sun, Q. Identification and characterization of wheat long non-protein coding RNAs responsive to powdery mildew infection and heat stress by using microarray analysis and SBS sequencing. *BMC Plant Biol.* **2011**, *11*, 61. [CrossRef] [PubMed]
23. Kim, E.-D.; Sung, S. Long noncoding RNA: Unveiling hidden layer of gene regulatory networks. *Trends Plant Sci.* **2012**, *17*, 16–21. [CrossRef] [PubMed]
24. Zhang, Y.-C.; Liao, J.-Y.; Li, Z.-Y.; Yu, Y.; Zhang, J.-P.; Li, Q.-F.; Qu, L.-H.; Shu, W.-S.; Chen, Y.-Q. Genome-wide screening and functional analysis identify a large number of long noncoding RNAs involved in the sexual reproduction of rice. *Genome Biol.* **2014**, *15*, 1–16. [CrossRef]
25. Uszczynska-Ratajczak, B.; Lagarde, J.; Frankish, A.; Guigó, R.; Johnson, R. Towards a complete map of the human long non-coding RNA transcriptome. *Nat. Rev. Genet.* **2018**, *19*, 535–548. [CrossRef]
26. Karlik, E.; Gözükırmızı, N. Evaluation of Barley lncRNAs Expression Analysis in Salinity Stress. *Russ. J. Genet.* **2018**, *54*, 198–204. [CrossRef]
27. Sun, Q.; Csorba, T.; Skourti-Stathaki, K.; Proudfoot, N.J.; Dean, C. R-Loop Stabilization Represses Antisense Transcription at the *Arabidopsis FLC* Locus. *Science* **2013**, *340*, 619–621. [CrossRef]
28. Ariel, F.; Jegu, T.; Latrasse, D.; Romero-Barrios, N.; Christ, A.; Benhamed, M.; Crespi, M. Noncoding Transcription by Alternative RNA Polymerases Dynamically Regulates an Auxin-Driven Chromatin Loop. *Mol. Cell* **2014**, *55*, 383–396. [CrossRef]
29. Wang, H.; Chung, P.J.; Liu, J.; Jang, I.-C.; Kean, M.J.; Xu, J.; Chua, N.-H. Genome-wide identification of long noncoding natural antisense transcripts and their responses to light in *Arabidopsis*. *Genome Res.* **2014**, *24*, 444–453. [CrossRef]
30. Ding, J.; Lu, Q.; Ouyang, Y.; Mao, H.; Zhang, P.; Yao, J.; Xu, C.; Li, X.; Xiao, J.; Zhang, Q. A long noncoding RNA regulates photoperiod-sensitive male sterility, an essential component of hybrid rice. *Proc. Natl. Acad. Sci. USA* **2012**, *109*, 2654–2659. [CrossRef]
31. Zhou, H.; Liu, Q.; Li, J.; Jiang, D.; Zhou, L.; Wu, P.; Lu, S.; Li, F.; Zhu, L.; Liu, Z.; et al. Photoperiod- and thermo-sensitive genic male sterility in rice are caused by a point mutation in a novel noncoding RNA that produces a small RNA. *Cell Res.* **2012**, *22*, 649–660. [CrossRef]
32. Dinger, M.E.; Pang, K.C.; Mercer, T.R.; Mattick, J.S. Differentiating Protein-Coding and Noncoding RNA: Challenges and Ambiguities. *PLoS Comput. Biol.* **2008**, *4*, e1000176. [CrossRef] [PubMed]
33. Zhang, J.; Mujahid, H.; Hou, Y.; Nallamilli, B.R.; Peng, Z. Plant Long ncRNAs: A New Frontier for Gene Regulatory Control. *Am. J. Plant Sci.* **2013**, *4*, 1038–1045. [CrossRef]
34. Liao, P.; Li, S.; Cui, X.; Zheng, Y. A comprehensive review of web-based resources of non-coding RNAs for plant science research. *Int. J. Biol. Sci.* **2018**, *14*, 819–832. [CrossRef] [PubMed]
35. Ausin, I.; Greenberg, M.V.C.; Simanshu, D.K.; Hale, C.J.; Vashisht, A.A.; Simon, S.A.; Lee, T.-F.; Feng, S.; Española, S.D.; Meyers, B.C.; et al. Involved in de NOVO 2-containing complex involved in RNA-directed DNA methylation in *Arabidopsis*. *Proc. Natl. Acad. Sci. USA* **2012**, *109*, 8374–8381. [CrossRef] [PubMed]
36. Li, L.; Eichten, S.R.; Shimizu, R.; Petsch, K.; Yeh, C.-T.; Wu, W.; Chettoor, A.M.; Givan, S.A.; Cole, R.A.; Fowler, J.E.; et al. Genome-wide discovery and characterization of maize long non-coding RNAs. *Genome Biol.* **2014**, *15*, R40. [CrossRef]
37. Zhu, B.; Yang, Y.; Li, R.; Fu, D.; Wen, L.; Luo, Y.; Zhu, H. RNA sequencing and functional analysis implicate the regulatory role of long non-coding RNAs in tomato fruit ripening. *J. Exp. Bot.* **2015**, *66*, 4483–4495. [CrossRef]
38. Liu, J.; Jung, C.; Xu, J.; Wang, H.; Deng, S.; Bernad, L.; Arenas-Huertero, C.; Chua, N.-H. Genome-Wide Analysis Uncovers Regulation of Long Intergenic Noncoding RNAs in *Arabidopsis*. *Plant Cell* **2012**, *24*, 4333–4345. [CrossRef]

39. Yang, T.; Ma, H.; Zhang, J.; Wu, T.; Song, T.; Tian, J.; Yao, Y. Systematic identification of long noncoding RNA s expressed during light-induced anthocyanin accumulation in apple fruit. *Plant J.* **2019**, *100*, 572–590. [CrossRef]
40. Liu, S.; Sun, Z.; Xu, M. Identification and characterization of long non-coding RNAs involved in the formation and development of poplar adventitious roots. *Ind. Crop. Prod.* **2018**, *118*, 334–346. [CrossRef]
41. Liu, S.; Wu, L.; Qi, H.; Xu, M. LncRNA/circRNA–miRNA–mRNA networks regulate the development of root and shoot meristems of Populus. *Ind. Crop. Prod.* **2019**, *133*, 333–347. [CrossRef]
42. Wierzbicki, A.T. The role of long non-coding RNA in transcriptional gene silencing. *Curr. Opin. Plant Biol.* **2012**, *15*, 517–522. [CrossRef] [PubMed]
43. Kornienko, A.E.; Guenzl, P.M.; Barlow, D.P.; Pauler, F.M. Gene regulation by the act of long non-coding RNA transcription. *BMC Biol.* **2013**, *11*, 1–14. [CrossRef] [PubMed]
44. Dykes, I.M.; Emanueli, C. Transcriptional and Post-transcriptional Gene Regulation by Long Non-coding RNA. *Genom. Proteom. Bioinform.* **2017**, *15*, 177–186. [CrossRef] [PubMed]
45. Qin, T.; Zhao, H.; Cui, P.; Albesher, N.; Xiong, L. A Nucleus-Localized Long Non-Coding RNA Enhances Drought and Salt Stress Tolerance. *Plant Physiol.* **2017**, *175*, 1321–1336. [CrossRef]
46. Depège, N.; Bellafiore, S.; Rochaix, J.-D. Role of Chloroplast Protein Kinase Stt7 in LHCII Phosphorylation and State Transition in *Chlamydomonas*. *Science* **2003**, *299*, 1572–1575. [CrossRef]
47. Dewir, Y.H.; Paek, K.Y. The control of in vitro flowering and association of glutathione metabolism. In *Plant Tissue Culture and Applied Plant Biotechnology*; Kumar, A., Roy, S., Eds.; Aavishkar Publishers: Jaipur, India, 2011; pp. 77–108.
48. Kang, C.; Liu, Z. Global identification and analysis of long non-coding RNAs in diploid strawberry Fragaria vesca during flower and fruit development. *BMC Genom.* **2015**, *16*, 1–15. [CrossRef]
49. Yu, S.; Galvão, V.C.; Zhang, Y.-C.; Horrer, D.; Zhang, T.-Q.; Hao, Y.-H.; Feng, Y.-Q.; Wang, S.; Schmid, M.; Wang, J.-W. Gibberellin Regulates the *Arabidopsis* Floral Transition through miR156-Targeted SQUAMOSA PROMOTER BINDING–LIKE Transcription Factors. *Plant Cell* **2012**, *24*, 3320–3332. [CrossRef]
50. Wu, H.-J.; Wang, Z.-M.; Wang, M.; Wang, X.-J. Widespread Long Noncoding RNAs as Endogenous Target Mimics for MicroRNAs in Plants. *Plant Physiol.* **2013**, *161*, 1875–1884. [CrossRef]
51. Luo, R.L.; Li, Y.X.; Zhang, J.; Zhang, J.; Yao, Y.C. Cloning and functional assay of McmiR160 regulated leaf coloration in *Malus* spp. *J. Beijing Univ. Agric.* **2019**, *34*, 14–19. (In Chinese)
52. Aung, B.; Gao, R.; Gruber, M.Y.; Yuan, Z.-C.; Sumarah, M.; Hannoufa, A. MsmiR156 affects global gene expression and promotes root regenerative capacity and nitrogen fixation activity in alfalfa. *Transgenic Res.* **2017**, *26*, 541–557. [CrossRef] [PubMed]
53. Zheng, Y.; Chen, K.; Xu, Z.; Liao, P.; Zhang, X.; Liu, L.; Wei, K.; Liu, D.; Li, Y.-F.; Sunkar, R.; et al. Small RNA profiles from Panax notoginseng roots differing in sizes reveal correlation between miR156 abundances and root biomass levels. *Sci. Rep.* **2017**, *7*, 9418. [CrossRef] [PubMed]
54. Barrera-Rojas, C.H.; Rocha, G.H.B.; Polverari, L.; Brito, D.A.P.; Batista, D.S.; Notini, M.M.; Da Cruz, A.C.F.; Morea, E.G.O.; Sabatini, S.; Otoni, W.C.; et al. miR156-targeted SPL10 controls Arabidopsis root meristem activity and root-derived de novo shoot regeneration via cytokinin responses. *J. Exp. Bot.* **2019**, *71*, 934–950. [CrossRef] [PubMed]
55. Meng, Y.; Shao, C.; Wang, H.; Jin, Y. Target mimics: An embedded layer of microRNA-involved gene regulatory networks in plants. *BMC Genom.* **2012**, *13*, 197. [CrossRef]
56. He, J.-H.; Han, Z.-P.; Zou, M.-X.; Wang, L.; Lv, Y.B.; Bin Zhou, J.; Cao, M.-R.; Li, Y.-G. Analyzing the LncRNA, miRNA, and mRNA Regulatory Network in Prostate Cancer with Bioinformatics Software. *J. Comput. Biol.* **2018**, *25*, 146–157. [CrossRef]
57. Zhang, G.; Chen, D.; Zhang, T.; Duan, A.; Zhang, J.; He, C. Transcriptomic and functional analyses unveil the role of long non-coding RNAs in anthocyanin biosynthesis during sea buckthorn fruit ripening. *DNA Res.* **2018**, *25*, 465–476. [CrossRef]
58. Datta, R.; Paul, S. Long non-coding RNAs: Fine-tuning the developmental responses in plants. *J. Biosci.* **2019**, *44*, 77. [CrossRef]
59. Wu, G.; Park, M.Y.; Conway, S.R.; Wang, J.-W.; Weigel, D.; Poethig, R.S. The Sequential Action of miR156 and miR172 Regulates Developmental Timing in Arabidopsis. *Cell* **2009**, *138*, 750–759. [CrossRef]
60. Martin, R.C.; Asahina, M.; Liu, P.-P.; Kristof, J.R.; Coppersmith, J.L.; Pluskota, W.E.; Bassel, G.W.; Goloviznina, N.A.; Nguyen, T.T.; Martínez-Andújar, C.; et al. The microRNA156 and microRNA172 gene regulation cascades at post-germinative stages in *Arabidopsis*. *Seed Sci. Res.* **2010**, *20*, 79–87. [CrossRef]
61. Cui, L.-G.; Shan, J.-X.; Shi, M.; Gao, J.-P.; Lin, H.-X. The *miR156-SPL9-DFR* pathway coordinates the relationship between development and abiotic stress tolerance in plants. *Plant J.* **2014**, *80*, 1108–1117. [CrossRef]
62. Lei, K.-J.; Lin, Y.-M.; Ren, J.; Bai, L.; Miao, Y.-C.; An, G.-Y.; Song, C.-P. Modulation of the Phosphate-Deficient Responses by MicroRNA156 and its Targeted squamosa promoter binding protein-like 3 in Arabidopsis. *Plant Cell Physiol.* **2015**, *57*, 192–203. [CrossRef] [PubMed]
63. Lei, K.J.; Lin, Y.M.; An, G.Y. miR156 modulates rhizosphere acidification in response to phosphate limitation in Arabidopsis. *J. Plant Res.* **2015**, *129*, 275–284. [CrossRef] [PubMed]
64. Zhang, X.; Zou, Z.; Zhang, J.; Zhang, Y.; Han, Q.; Hu, T.; Xu, X.; Liu, H.; Li, H.; Ye, Z. Over-expression of sly-miR156a in tomato results in multiple vegetative and reproductive trait alterations and partial phenocopy of the *sft* mutant. *FEBS Lett.* **2010**, *585*, 435–439. [CrossRef] [PubMed]

65. e Silva, G.F.F.; Silva, E.M.; Azevedo, M.D.S.; Guivin, M.A.C.; Ramiro, D.A.; Figueiredo, C.R.; Carrer, H.; Peres, L.E.P.; Nogueira, F.T.S. microRNA156-targeted SPL/SBP box transcription factors regulate tomato ovary and fruit development. *Plant J.* **2014**, *78*, 604–618. [CrossRef]
66. Li, K.; Wei, Y.-H.; Wang, R.-H.; Mao, J.-P.; Tian, H.-Y.; Chen, S.-Y.; Li, S.-H.; Tahir, M.-M.; Zhang, D. Mdm-MIR393b-mediated adventitious root formation by targeted regulation of MdTIR1A expression and weakened sensitivity to auxin in apple rootstock. *Plant Sci.* **2021**, *308*, 110909. [CrossRef]
67. Li, X.; Chen, P.; Xie, Y.; Yan, Y.; Wang, L.; Dang, H.; Zhang, J.; Xu, L.; Ma, F.; Guan, Q. Apple SERRATE negatively mediates drought resistance by regulating MdMYB88 and MdMYB124 and microRNA biogenesis. *Hortic. Res.* **2020**, *7*, 1–11. [CrossRef]
68. Xue, T.; Liu, Z.; Dai, X.; Xiang, F. Primary root growth in Arabidopsis thaliana is inhibited by the miR159 mediated repression of MYB33, MYB65 and MYB101. *Plant Sci.* **2017**, *262*, 182–189. [CrossRef]
69. Matthewman, C.A.; Kawashima, C.G.; Huska, D.; Csorba, T.; Dalmay, T.; Kopriva, S. miR395 is a general component of the sulfate assimilation regulatory network in Arabidopsis. *FEBS Lett.* **2012**, *586*, 3242–3248. [CrossRef]
70. Ferdous, J.; Whitford, R.; Nguyen, M.; Brien, C.; Langridge, P.; Tricker, P.J. Drought-inducible expression of Hv-miR827 enhances drought tolerance in transgenic barley. *Funct. Integr. Genom.* **2016**, *17*, 279–292. [CrossRef]
71. Xu, J.; Li, C.; Cui, L.; Zhang, T.; Wu, Z.; Zhu, P.-Y.; Meng, Y.-J.; Zhang, K.-J.; Yu, X.-Q.; Lou, Q.-F.; et al. New insights into the roles of cucumber TIR1 homologs and miR393 in regulating fruit/seed set development and leaf morphogenesis. *BMC Plant Biol.* **2017**, *17*, 130. [CrossRef]
72. Wang, Y.C.; Xu, H.F.; Wang, N.; Jiang, S.H.; Liu, J.X.; Wang, D.Y.; Zuo, W.F.; Chen, X.S. Molecular cloning and expression analysis of an auxin signaling related gene MdARF3 in red flesh apple. *Acta Hortic. Sin.* **2017**, *44*, 633–643. [CrossRef]
73. Pertea, M.; Kim, D.; Pertea, G.M.; Leek, J.T.; Salzberg, S.L. Transcript-level expression analysis of RNA-seq experiments with HISAT, StringTie and Ballgown. *Nat. Protoc.* **2016**, *11*, 1650–1667. [CrossRef] [PubMed]
74. Mao, X.Z.; Cai, T.; Olyarchuk, J.G.; Wei, L.P. Automated genome annotation and pathway identification using the KEGG Orthology (KO) as a controlled vocabulary. *Bioinformatics* **2005**, *21*, 3787–3793. [CrossRef] [PubMed]
75. Shannon, P.; Markiel, A.; Ozier, O.; Baliga, N.S.; Wang, J.T.; Ramage, D.; Amin, N.; Schwikowski, B.; Ideker, T. Cytoscape: A software environment for integrated models of Biomolecular Interaction Networks. *Genome Res.* **2003**, *13*, 2498–2504. [CrossRef] [PubMed]
76. Yin, J.L.; Fang, Z.W.; Sun, C.; Zhang, P.; Zhang, X.; Lu, C.; Wang, S.P.; Ma, D.F.; Zhu, Y.X. Rapid identification of a stripe rust resistant gene in a space-induced wheat mutant using specific locus amplified fragment (SLAF) sequencing. *Sci. Rep.* **2003**, *8*, 3086. [CrossRef] [PubMed]